Journal of
Applied
Crystallography
ISSN 0021-8898

Received 22 February 2007
Accepted 21 June 2007

# Methods for obtaining the strain-free lattice parameter when using diffraction to determine residual stress

**P. J. Withers,[a]* M. Preuss,[a] A. Steuwer[b] and J. W. L. Pang[c]**

[a]Materials Science Centre, School of Materials, Manchester University, Grosvenor Street, Manchester M1 7HS, UK, [b]FaME38 at the ILL/ESRF, 6 rue J. Horowitz, 38042 Grenoble Cedex, France, and [c]Materials Science and Technology Division, Oak Ridge National Laboratory, PO Box 2008, Oak Ridge, Knoxville, Tennessee, TN 37831-6118, USA. Correspondence e-mail: philip.withers@manchester.ac.uk

The determination of residual stress by diffraction depends on the correct measurement of the strain-free lattice spacing $d^0_{hkl}$, or alternatively the enforcement of some assumption about the state of strain or stress within the body. It often represents the largest uncertainty in residual stress measurements since there are many ways in which the strain-free lattice spacing can vary in ways that are unrelated to stress. Since reducing this uncertainty is critical to improving the reliability of stress measurements, this aspect needs to be addressed, but it is often inadequately considered by experimenters. Many different practical strategies for the determining of $d^0_{hkl}$ or $d_{\rm ref}$ have been developed, some well known, others less so. These are brought together here and are critically reviewed. In practice, the best method will vary depending on the particular application under consideration. Consequently, situations for which each method are appropriate are identified with reference to practical examples.

© 2007 International Union of Crystallography
Printed in Singapore – all rights reserved

## 1. Introduction

Residual stress is the stress that remains in a body that is stationary when all applied stresses have been removed. It is important because it can combine with applied stresses to cause failure at levels below that at which failure would occur from the applied stresses alone. Because they are self-equilibrating, unlike applied stresses, residual stress cannot be calculated from the forces, impulses and couples experienced by a material, component or assembly. In a polycrystalline material, residual stresses manifest themselves in the form of residual elastic strains, which depend on the elastic and plastic properties of the materials, and which can be, like stresses, expressed by tensors. Stresses and strains are related to each other by a constitutive material law. In the elastic regime, this is the generalized Hooke law, which relates strain to stress using certain elastic constants (Nye, 1985).

All diffraction-based measurements of elastic strain, $\varepsilon_{hkl}$, and hence residual stress, are based on a comparison of *hkl* lattice plane spacings measured in one or more directions for the region of interest, $d_{hkl}$, with a reference value, $d_{\rm ref}$ (= $d^0_{hkl}$),

$$\varepsilon_{hkl} = (d_{hkl} - d^0_{hkl})/d^0_{hkl}. \qquad (1)$$

The reference can be determined either in a 'stress-free' sample of identical material, deduced from other measurements, or by enforcing mechanical equilibrium conditions. Given that small changes in lattice parameter can give rise to very large changes in stress, in many cases attention is focused on the strained state with insufficient time paid, or effort expended, in obtaining reliable estimates of $d^0_{hkl}$. Furthermore, there are many other factors that can have an effect on the lattice spacing that are unrelated to stress. These factors, such as local changes in alloy chemistry, can give rise to changes in lattice parameter far greater than those that arise from residual stress. If unaccounted for these can seriously undermine the reliability of the stress measurement, potentially leading to catastrophic structural integrity assessment. Such effects are particularly difficult to account for without direct measurements if they cause the strain-free lattice spacing to vary from point to point throughout the body of interest.

On the other hand, in some cases it may not be necessary to actually measure a reference *d* spacing at all. For example, if it is known that a component of stress is strictly zero, this may be used to circumvent the need for an accurate $d^0_{hkl}$ value. The boundary condition that the normal stress component at a free surface must be zero is used extensively in laboratory-based X-ray investigations of near-surface stress fields, forming the basis of the so-called $\sin^2\psi$ technique (*e.g.* Eigenmann & Macherauch, 1995). If only the deviatoric stress is required, any reference *d* spacing can be used. The average of the three diagonal strain components ($\varepsilon_{11}$, $\varepsilon_{22}$, $\varepsilon_{33}$) measured relative to this arbitrary reference can then be subtracted from the diagonal elements of the measured strain tensor to yield the traceless deviatory strain tensor.

Methods for determining $d^0_{hkl}$ have been around since the 1940s (Durer, 1946; Glocker, 1951), as summarized by Hauk (1997) for the X-ray method. Despite the fact that a number of new methods have emerged recently, no further attempts have been made to review critically the merits and weaknesses of the different methods and to examine situations when each are appropriate. That is the purpose of this paper. The methods reviewed are not exhaustive but represent the most commonly applied techniques.

## 2. The 'strain-free' lattice parameter

Although the reference lattice spacing is often termed a 'stress-free' $d$ spacing, this only corresponds to a 'strain-free' spacing in the full triaxially stress-free case when all three principal values of the macroscopic stress and strain tensors are zero. There are cases when one component of the stress tensor may be zero, and therefore 'stress-free', but the corresponding strain component is not 'strain-free', as in the case of the out-of-plane strain component at a free surface (plane stress). The case of plane strain represents the converse example, where the out-of-plane lattice spacing is strain- but not stress-free. The $hkl$ lattice spacing can be determined from a single diffraction peak, or the 'average' lattice constants $a$, $b$ and $c$ can be obtained by refinement from multiple peaks, usually using a Rietveld refinement (Daymond *et al.*, 1997).

### 2.1. Statistics and uncertainties

The uncertainty in the strain-free lattice parameter will add to the uncertainty in the determined stresses. Since the value of the reference $d$ spacing occurs in the calculation of every component of the strain tensor, it is essential to spend adequate time on its measurement in order to determine its value with sufficient accuracy. It has been suggested (Johnson, 2005) that ten times the time used to acquire the other data points should be allocated to its measurement, so that it has an uncertainty three times that for the strained lattice spacing measurements themselves. It should also be remembered that the uncertainty in the reference $d$ spacing should not be added in quadrature to that associated with each $d$-spacing measurement unless a reference $d$ spacing is measured independently for each point, because any error will affect the strain recorded at each point systematically in the same manner rather than independently. This should also be remembered when combining strain measurements from different directions to calculate stress.

## 3. Factors that affect the strain-free lattice parameter

In view of the fact that in the uniaxial case an elastic strain of only $5 \times 10^{-4}$ represents a stress of 100 MPa in steel, stress-free changes in lattice spacing need to be anticipated and properly accounted for. There are many factors that can give rise to changes of such a magnitude, both on a local and on a global scale, some of which are listed below.

### 3.1. Compositional changes

Even slight changes in composition can bring about large changes in lattice spacing. For example, every 0.1 wt% of carbon in solution in steel can change the lattice parameter by $-51 \times 10^{-4}$ in ferrite and $+92 \times 10^{-4}$ in austenite (Bhadeshia *et al.*, 1991). Changes in solute content can be brought about by the precipitation or dissolution of second phases during heat treatment, for example during welding, or by segregation during casting. These can cause a steep variation in strain-free lattice spacing with position which can be an important problem in many practical cases, especially for heat-treatable alloys (see for example §§4.6.2 and 4.6.3). From an engineering point of view, aluminium alloys are among the most important heat-treatable alloys and the effects of solutes on the lattice spacing of aluminium (Mohr & Priesmeyer, 1995) are shown in Fig. 1. Solute changes can occur across similar length scales to the stress fields of interest: for example, in welded structures where localized heating is responsible for both the residual stress and the variations in solute content. Unless accounted for these prevent the accurate derivation of strains from measures of $d$ spacing and hence stresses. As a result it is probably prudent to assume that a change in the elastic strain-free lattice spacing may have occurred whenever a region of interest has experienced a thermodynamically significant thermal excursion, unless there is direct evidence to the contrary.

Local changes in composition are sometimes deliberately introduced, for example by doping in electronics to modify the electrical properties, or by carburization (Bourke *et al.*, 1998) and nitridation in steel.

### 3.2. Martensitic phase transformations

As discussed in §3.1, phase changes may cause compositional changes in the solute content in the matrix phase which are non-uniform across a sample owing to element partitioning rendering a global reference $d^0$ spacing inappropriate. Additionally, martensitic phase transformations can generate interphase stresses which mean that the $d$ spacing for one

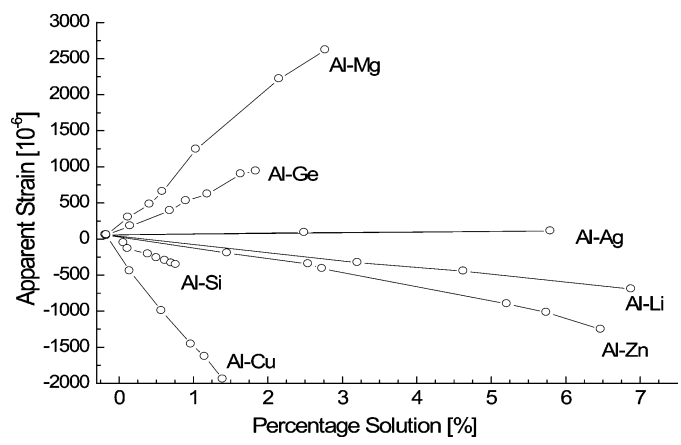


**Figure 1**
The variation (expressed in microstrain) of the unstrained lattice parameter with solute content for different solute elements (Johnson *et al.*, 1997) in aluminium (Barrett & Massalski, 1966).

**Table 1**
Summary of the various methods for obtaining an estimate of $a^0$.

| Method | Local or global | Determined or implied | Validity |
|---|---|---|---|
| Reference standard | Global | Determined | Absolute lattice spacings are not generally sufficiently well determined on strain mapping instruments |
| Filings/powders | Global | Determined | Often applicable for ceramics; only valid for metals if filings are representative of the alloy condition in the component |
| Cubes | Local | Determined | May retain intergranular stresses; vulnerable to geometrical effects if poorly positioned |
| Multiple measurements | Local | Determined | Absolute lattice spacings are generally well determined; measurements are relatively time-consuming |
| Triaxial X-ray | Local | Determined | Technically difficult to measure $d^0_{hkl}$ absolutely; must ensure identical sample–source distance for all measurements |
| Extrapolation using anisotropic reflections | Local | Implied | Only effective if crystal is reasonably elastically anisotropic and two stress states can be imposed (one could be as-received); is liable to errors when plasticity can occur between the two stress states |
| Far field | Global | Determined | Only valid if there is no spatial variation in $d^0_{hkl}$ and the variation for *hkl* is representative of the macrostress, and if chosen locations are actually stress-free |
| $\sin^2\psi$ | Local | Implied | Only valid for truly plane stress (nevertheless, there are many cases when this holds, *e.g.* near surface, in thin plates/slices); sensitive to intergranular and interphase stresses which may not be zero over the sampling volume, even when macrostress is zero |
| Stress balance | Global | Implied | Only valid if there is no spatial variation in $d^0_{hkl}$ and the complete area normal to the stress is mapped; variation for $a_{hkl}$ must be representative of the macrostress; best held in reserve as a confirmation that $a^0$ has been correctly estimated |

phase may not be stress-free even when the sample is macroscopically free of stress. Martensitic phase transformations can occur, for example, when a sample has undergone temperature changes, such as during welding, or under stress (superelastics) or electric field (ferroelectrics). Indeed, generally it is not wise to use measurements made on only one phase to represent the stress in the material as a whole unless the other phases are in a strong minority. However, from a practical point of view, it is not always possible to measure several peaks.

### 3.3. Changes in temperature

Any variation in temperature will give rise to stress-free changes in lattice spacing. Typically for metals a change in temperature of 1 K gives a fractional change in lattice spacing, or apparent strain, of the order of $10^{-5}$. As a result a 10 K change in fluctuation in temperature when measuring the sample being investigated and the reference spacing can be significant. For materials having crystal structures not belonging to cubic crystal systems, changes in temperature can also lead to thermally induced intergranular stresses owing to anisotropic thermal expansion, *e.g.* zirconium alloys (Gloaguen *et al.*, 2004).

### 3.4. Geometrical effects

When making diffraction measurements in the absence of an analyser crystal, geometrical effects associated with partial filling of the gauge volume (the nominal sampling volume defined by the incident and diffracted beam) can give rise to anomalous shifts in measured diffraction angles and thus give spurious stress-free strains (Hutchings *et al.*, 2005). These can have serious implications when measuring $d^0$ if for example small stress-free cubes are measured without meticulous positioning.

### 3.5. Intergranular strains

Intergranular (type II) strains can occur by crystallographically heterogeneous plastic deformation. As a result grain *hkl* families may be stressed even though the sample as a whole is unstressed. If not avoided or accounted for these 'pseudo-strains' may give an unrepresentative measure of the strain-free reference. They can exist and vary on a length scale similar to the grain size and so can remain even in the relatively small blocks of material used as 'stress-free' samples (see §4.3). Before choosing a measurement method it is thus important to decide whether the absolute or the macroscopically strain-free lattice spacing is required as the best reference. If the macrostress is of interest, in regions containing plastically or thermally generated intergranular stresses the latter can be more appropriate. This is because the difference between the lattice spacing before excision, and the reference spacing measured for the same region of interest after excision, is proportional to the macrostress, in that the type II stress is not relieved by excision.

## 4. Methods for determining a representative strain-free reference

In the guidelines agreed for residual stress measurement by neutron diffraction (Webster, 2001) the following methods were recommended:

(i) measurement at a position (*e.g.* a far-field region) or time known to contain negligible stress;

(ii) measurement on a stress-free powder or filings that are representative of the material being examined;

(iii) cutting stress-free reference cubes or combs from the sample;

(iv) application of force/moment balance.

Alternatively, it may be possible to infer the strain-free reference by imposing a zero stress condition perpendicular to a free surface, from the anisotropic behaviour of the various reflections or from the distortion of the diffraction cones. All

these methods are summarized in Table 1 and discussed in the following sections. Note that global methods only apply in cases where the application of a single global value of $d_{\rm ref}$ is valid.

### 4.1. Reference standard

While in principle it would be possible to measure the lattice spacing absolutely after calibrating the diffractometer with a standard sample, insufficient absolute accuracy of strain measurement instruments makes this a poor way to determine the strain-free lattice parameter. Besides, the available book values of stress-free lattice spacings are not usually reliable to sufficient accuracy ($\sim 10^{-5}$ strain) and, except in very few cases, the level of process control and repeatability is not good enough to eliminate compositional effects and other factors affecting the strain-free reference. As a consequence, this method is not considered a serious option for strain measurements.

### 4.2. Option 1: powders, filings, cubes and combs

By their very nature, fine powders and filings (Fig. 2*a*) cannot sustain a long-range macrostress and so provide ideal macrostress-free reference materials. The powder approach is attractive in the sense that powders are easy to handle in suitable containers. However, they should be measured at the same temperature (Ceretti *et al.*, 1998) (see §3.3) and should completely fill the instrumental gauge volume, or be very accurately centred at the instrument reference point, in order to avoid any geometrical shift in measured diffraction angle (§3.4). Additionally, any absorption in the powder may move the effective centroid of the gauge volume away from the reference point (Withers *et al.*, 2000).

Powder methods are particularly well suited to ceramics in that the constituent powder or particulate from which the component of interest was originally formed may be available. For metallic alloys, metal filings may be appropriate in certain cases, but they will almost certainly contain different intergranular strains (§3.5) from the component, which may mean that a given *hkl* reflection is neither completely stress-free nor representative of the intergranular residual stresses in the component.

By excision, either from the sample under investigation or a duplicate, a region can be freed from the constraint of the surrounding macroscopic stress field to provide a measure of $d_{\rm ref}$. Several methods of obtaining such samples can be used, including the cutting of small reference cubes, matchsticks or 'combs' (Fig. 2*b*), either taken from an identical component to that being measured or taken destructively from the same sample once the macrostressed lattice parameter has been mapped. Clearly a basic assumption of this method is that the stress field of interest is totally relaxed by the cutting procedure. The shorter the range of the stress field the finer the sample must be sectioned to relieve the stress.

Generally cubes are used, the smaller the better as long as the grain size is sufficiently small that powder average conditions are maintained. However, compared with the powder approach, small cubes are difficult to handle and to position accurately at the instrument reference point. If there is a variation in composition in the sample, the reference strain-free lattice spacings, $d^0$, must be measured at exactly the locations of the strain data points themselves. This calls for an extensive process of extracting small reference cubes, for example across a weld region, and subsequently measuring them individually. A practical example of this cumbersome method is given by Krawitz & Winholtz (1994), who showed that in their case it was necessary to obtain individual reference values for each location in question.

Typically, type I stresses (macrostresses) are relieved by excising small cubes or matchsticks (if the stress is expected to vary slowly in the extended direction), but type II (grain-scale intergranular) and type III (atomic scale) stresses are retained by the cutting procedure. In some respects this can be an advantage of the technique in that the difference between $d_{hkl}(x, y, z)$ and the measured $d_{\rm ref}(x, y, z)$ is directly proportional only to the macrostress because the type II stresses have remained unchanged. A good example of the evaluation of $d^0$

(*a*)

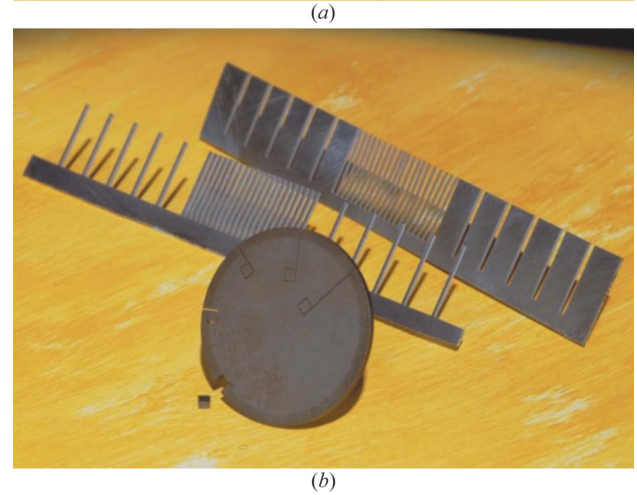

(*b*)

**Figure 2**
Powders, 'cubes' and combs for the determination of strain-free reference values. (*a*) Powder along with a powder sample can; stress-free cubes and a typical tensile specimen. (*b*) A 'comb' and its 'negative' cut at mid-plate thickness with the teeth parallel to the welding direction of an Al friction stir weldment, and a disc-like structure cut from a steel automotive crank shaft from which a series of small stress-free reference cubes are being cut at different radial distances (Hutchings *et al.*, 2005).

with position is given by the excision of matchstick reference samples (2 × 2 × 16 mm with the long axis along the weld) from a mock-up double 'V' weldment joining two ~780 mm-diameter 16 mm-thick type 316 stainless-steel tubes (Fig. 3*a*). This procedure was necessary because, depending on their proximity to the weld, different regions experienced different localized heat treatments and an estimate of the triaxial stress near the weld line was required (Hutchings *et al.*, 2000). The matchsticks were cut from the weldment by a 'stress-free' electro-discharge machine technique at various positions local to the weld (Fig. 3) including a set at different axial distances ($z$) each located 2 mm from the outer surface. The diffraction peaks for various *hkl* planes oriented at 45° to the radial-axial directions of the cylinder were measured for each matchstick on the ENGIN instrument (Johnson *et al.*, 1997) at ISIS, Rutherford Appleton Laboratories, UK. Both a full Rietveld analysis using all the diffraction peaks, and separate analyses of four individual diffraction peaks (111, 200, 022 and 311), were carried out for each matchstick. Lattice 'strains' in the matchstick samples were determined with reference to measurements of $d_{\rm ref}$ made at a far-field point 48 mm from the weld centre line, taken to be at zero strain: that is, strains at this location were assumed to be unaffected by local compositional variations or by plastic strain-induced residual microstresses. The results of a hardness survey confirmed that no significant plastic strain had been induced this far from the weld.

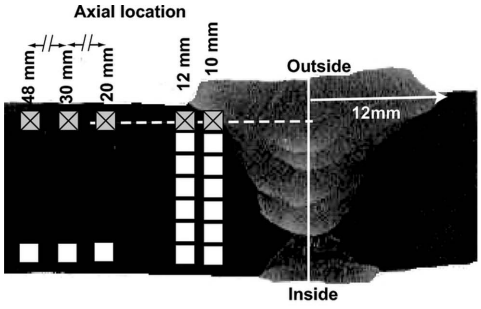


(*a*)

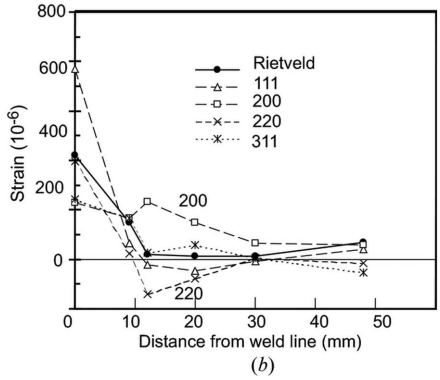


(*b*)

**Figure 3**
(*a*) A double 'V' butt weld joining two 16 mm-thick AISI Type 316L austenitic steel pipes. Squares denote positions at which 2 × 2 × 16 mm 'matchstick' samples were taken. (*b*) 'Pseudo-strains' measured in the 'matchstick' samples taken from positions [crossed squares in (*a*)] away from the weld along a line 2 mm below the outer surface (Hutchings *et al.*, 2000).

The measured strains for the matchsticks are shown in Fig. 3(*b*). Except in the weld itself ($z$ < 12 mm), where compositionally induced changes in $d^0$ are evident, the 'strains' determined from the Rietveld analysis are negligible. This is consistent with the notion that the Rietveld lattice parameter is representative of the macrostress in relatively untextured material because it averages the response over many reflections (Daymond *et al.*, 1997). However, in the heat-affected zone (12 mm > $z$ > 30 mm), considerable intergranular strains are evident as a function of *hkl*. These are most probably due to plastic intergranular strains. Consistent with *in situ* tensile test observations these deviations are most marked for the 200 reflection and least for the 111 reflection (Hutchings *et al.*, 2005). This is characteristic of plastic anisotropy in stainless steel, with 200 exhibiting the largest intergranular strains and 220 smaller strains in the opposite sense (Clausen *et al.*, 1999). It is seen that the variations in strain from these peaks bound the Rietveld curve in both the weld and the heat-affected zone. In the proposed stress measurement standard for neutron strain measurement (Webster, 2001) use of 111, 311 or 422 is recommended when making macrostrain measurements in plastically strained (fcc) stainless steel, whereas 200 is advised against because of its sensitivity to intergranular strain.

It is clear from these results that if single diffraction peak measurements of $d^0$ from small cut reference samples are used as the 'zero strain' reference they will incorporate a contribution from residual intergranular strains, if plasticity has occurred. Provided the extent of plasticity is exactly the same as that in the original sample they will have essentially the same intergranular strain. As a result, the use of $d^0$ measured in the same locations will give the correct macrostress-related elastic lattice strains, since the intergranular strains, as well as any compositional variations in sample and reference, will cancel out. However if a far-field zero strain reference $d^0$ is used, the possibility for intergranular strains in the measurements on the sample must be allowed for in the analysis.

An elegant alternative approach, suitable in appropriate circumstances, is to manufacture so-called reference 'combs' from a notionally identical reference sample, examples of which are shown in Fig. 2(*b*). The comb should be cut in an orientation appropriate for the expected stress state. The 'comb' design is effective when it is anticipated that no steep variation in $d^0$ is expected in the direction chosen to be the 'long' axis of the 'teeth', for example parallel to the welding direction for a weldment. In such cases, because the stress changes only over relatively long distances, the long axis of the tooth does not inhibit stress relaxation. The teeth are thus rendered almost free from the constraint of the surroundings, but left in registry through a small mechanical connection to the base material. Such structures circumvent the problems associated with handling small reference cubes and at the same time retain the positional relationship between each 'tooth'. In Fig. 2(*b*) the teeth are more closely spaced in the near weld region for better spatial resolution.

### 4.3. Option 2: using multiple measurements

One way to determine a representative strain-free lattice parameter is by averaging multiple measurements from a reference sample. Small coupons from the original material or the stressed sample itself are used for this method. The net intergranular strain averaged over all grain orientations in the coupon must be zero and any macroscopic stress must have been relieved by cutting a small coupon. If lattice spacings of various reflections are measured along as many sample directions as possible, then their corresponding lattice parameters $d_{hkl}$ are likely to average out to give a strain-free $a^0$.

The reliability of this method is demonstrated through measurements on Al7050 (Pang *et al.*, 1998). A tensile sample was prepared from an Al7050 rolled plate. The sample was strained to 2% plastic deformation by uniaxial tension. The generation of the intergranular strains for various *hkl* reflections was measured by neutron diffraction. The strain-free lattice parameter $a^0$ was determined from a small coupon of $\sim 5 \times 5 \times 10$ mm removed from the original rolled plate as a reference sample. A second coupon was cut out from the deformed sample after the tensile test. The same scheme of measurements was made on both samples. In principle, the global stress-free lattice parameter obtained from both the reference and the deformed samples should agree within experimental errors. All the neutron diffraction measurements were carried out on the spectrometer E3 at the NRU reactor in Canada.

The entire sample volume was irradiated in the measurements to ensure zero macrostress and because intergranular strain is an intensive quantity which for uniform straining is independent of spatial position. The intergranular strain is a function of grain orientations with respect to the sample coordinates, however, and different strain responses are expected among grains with different normal vectors along a given sample direction. Lattice spacings for the 222, 200, 220 and 311 reflections were measured at 15° intervals over a quadrant of a hemisphere. The spherical coordinate system ($\eta$, $\chi$) was used to describe the angular position, where $\eta$ is the angle between the transverse axis ($x$) of the sample and the projection of the angular position of interest (POI) on the transverse plane, and $\chi$ is the angle between the vertical sample axis ($z$) and the POI. The strain-free lattice parameter $a^0$ of the plate was determined by averaging measurements of all the measured reflections and sample orientations.

Plots of the lattice parameter for the reference sample and the deformed sample for the different reflections are shown in Figs. 4 and 5, respectively. The deformed sample shows a larger distribution of lattice parameters, particularly for the reflection 200. This is not surprising as the 200 reflection is known for its relatively large intergranular strains (Webster, 2001). Nevertheless, the two samples show the same average lattice parameter to within the experimental error, $a^0$ = 4.0508 (1) Å, consistent with the assumption that a reliable estimate of the strain-free lattice parameter can be obtained by averaging measurements for multiple reflections and sample directions.

It should be noted that this method provides an estimate of the absolutely strain-free lattice parameter $a^0$. The difference between this value and one of the macroscopically, but not microscopically, strain-free measurements $d^0_{hkl}$ ($\eta$, $\chi$) in Fig. 4 or Fig. 5 represents the intergranular strain in the coupon in that direction for *hkl*. If only the macrostress is of interest $d^0_{hkl}$ ($\eta$, $\chi$) may be more appropriate.

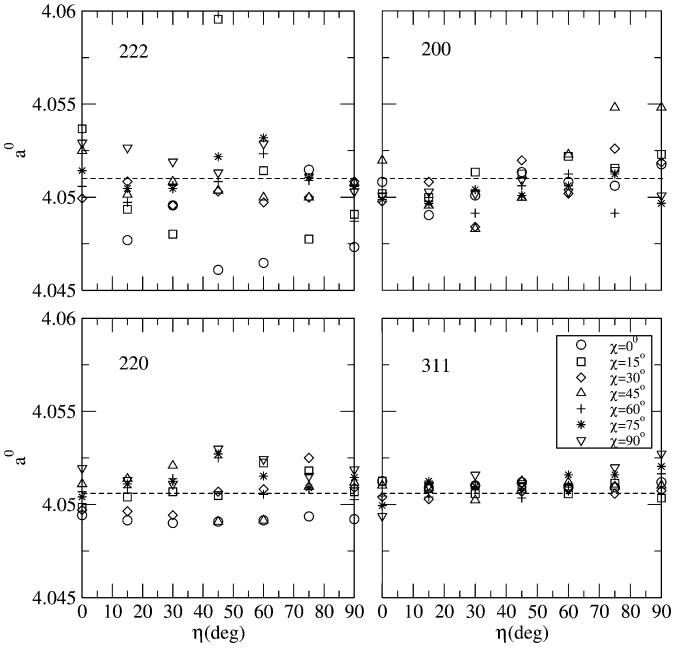


**Figure 4**
Variation of lattice parameters of the reference sample for reflections 222, 200, 220 and 311 plotted as a function of $\eta$ and $\chi$. The dotted line is the value of the stress-free lattice parameter.

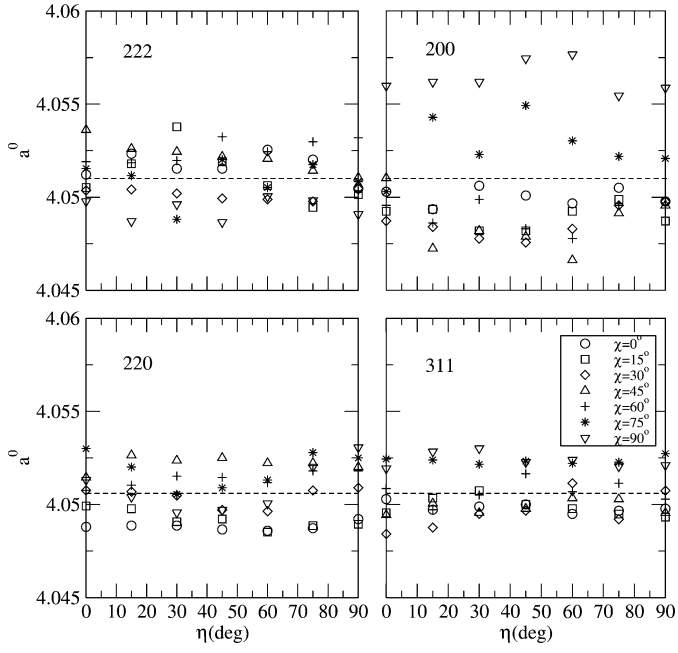


**Figure 5**
Variation of lattice parameters for a plastically deformed sample for reflections 222, 200, 220 and 311 plotted as a function of $\eta$ and $\chi$. The dotted line is the value of the stress-free lattice parameter.

### 4.4. Option 3: extrapolation using anisotropic reflections

This method for the calculation of a stress-free lattice parameter from the analysis of diffraction data from stressed material utilizes the elastic anisotropy of the material to infer $d^0$ and was developed by Daymond & Johnson (2001). The method relies on the fact that the lines describing the variation in lattice parameter with stress corresponding to two reflections $h_1k_1l_1$ and $h_2k_2l_2$ defined by the points $\{\sigma^1, a_{h_1k_1l_1}\}$, $\{\sigma^2, a_{h_1k_1l_1}\}$ and $\{\sigma^1, a_{h_2k_2l_2}\}$, $\{\sigma^2, a_{h_2k_2l_2}\}$ intersect at a value of '$a$' that is independent of the values of $\sigma^1$ and $\sigma^2$ (Fig. 6$a$). Consequently, an ignorance of the actual stress values ($\sigma^1$, $\sigma^2$) is no bar to determining the value of $a^0$ at which the stress is zero. The only requirement is that the lattice parameters for the two reflections $h_1k_1l_1$ and $h_2k_2l_2$ are recorded at the same (arbitrary) stress values. The value of $a^0$ is then given by

$$a^0 = (a_{h_1k_1l_1}a_{h_2k_2l_2} - a_{h_2k_2l_2}a_{h_1k_1l_1}) \times (a_{h_1k_1l_1} + a_{h_2k_2l_2} - a_{h_2k_2l_2} - a_{h_1k_1l_1}). \quad (2)$$

The technique is demonstrated in Fig. 6($a$) using data obtained during a uniaxial tension test on untextured austenitic (face-centred cubic) steel using the 111 and 200 reflections (Daymond & Johnson, 2001). Clearly, the uncertainty in the value of $a^0$ thus determined depends on the difference in gradients of the two lines (*i.e.* the larger the difference in diffraction elastic constants between the two reflections the better) and the difference between the two stress levels. The uncertainties in the calculated lattice parameter for various choices of number of diffraction peaks and different number of stress levels available for the calculation are shown in Fig. 6($b$). This indicates that, when all the data are within the elastic regime, an accurate evaluation of the reference lattice parameter can be made. When some data are in the plastic regime, a more limited evaluation is possible. In other words, the results suggest that, for cubic materials at least, the measurement of lattice parameters from a minimum of two different diffraction peaks at a minimum of two arbitrary stress values allows a stress-free lattice parameter ($a^0$) to be calculated. This is possible even if the stress values and the individual diffraction elastic constants for the two diffraction planes are unknown. A more general analysis is possible using many diffraction peaks and multiple stress levels, providing improved accuracy.

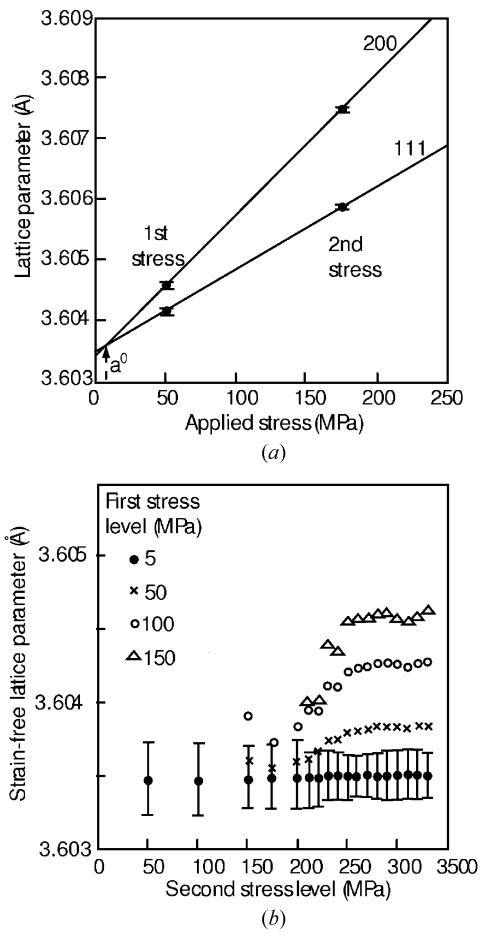


**Figure 6**
($a$) The determination of the stress-free lattice parameter inferred from the spacings for 111 and 200 at 50 and 175 MPa for austenitic steel. ($b$) The corresponding variation in uncertainty in $a^0$ according to first ($\sigma^1$) and second ($\sigma^2$) stress levels at which the lattice spacings for 111 and 200 are determined (Daymond & Johnson, 2001).

### 4.5. Option 4: measurement in a region known to be free of macrostress

A common approach is to use a far-field value of $d$ spacing as a reference. This reference must be measured in a region of the sample that is considered to be unlikely to be affected by the process from which the residual stress field in question originated. Note that this method of globally fixing $d^0$ is not appropriate in cases where there may be localized heating, such as near a weld, because of the possible local compositional changes discussed in §3. An illustrative example of where this technique might be applied is the strain field around a rivet holding together two plates. Because the stress field is mechanically induced and would be expected to fall off rapidly with distance from the rivet, a representative far-field $d_{\rm ref}$ can be obtained as far away from the rivet as possible (assuming there is no other source of residual stress), and the reference level is established by averaging the $d$ spacing measured through thickness (*e.g.* to ensure any quenching stresses are accounted for) or by averaging over a number of orientations. An example is shown in Fig. 7, which shows the strains measured with radial location from a 2124 Al rivet holding together two 7010 Al plates. Strictly, stress balance should be applied to check that the far-field region is indeed in a state of low stress. That this is the case here is evident from the good agreement with the finite element model, which necessarily obeys stress balance.

### 4.6. Option 5: exploitation of plane stress or plane strain conditions

There are many methods that rely on some assumptions about the state of stress, or strain, to infer the strain-free lattice spacing or in-plane stress. Of these, the $\sin^2\psi$ method is the most commonly applied, being a very powerful and versatile technique which has found widespread application in

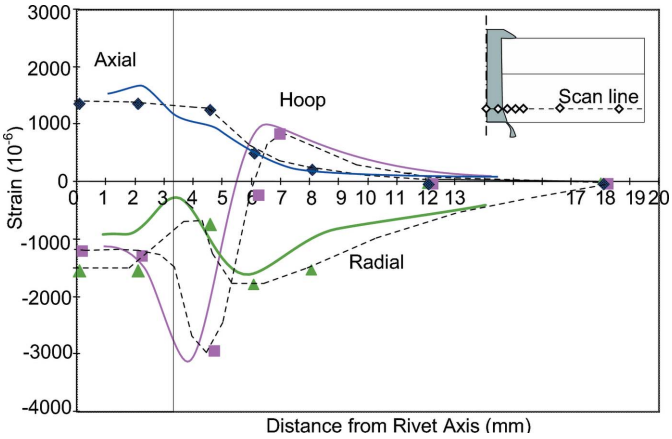


**Figure 7**
The axial, radial and hoop strains (solid symbols) measured 3 mm below the surface by neutron diffraction at positions (open diamonds) radially from the axis of a 3 mm radius 2124 Al rivet joining two 7010 Al plates (see inset). The rivet spacing was 30 mm and the strain-free $d^0$ value was measured laterally towards the edge of the plate, far from the line of rivets. The continuous lines represent the predictions from a finite element model smeared to match the spatial resolution of the sampling gauge. The good agreement with the data validates the use of the far-field measurement of $d^0$.

laboratory X-ray-based stress measurement. It is based on the general stress–strain relationship for an elastically isotropic material (*e.g.* Noyan & Cohen, 1987):

$$\begin{aligned}\varepsilon_{\varphi\psi} &= \frac{d_{\varphi\psi} - d^0}{d^0} \\ &= \frac{1+\nu}{E}\left(\sigma_{11}\cos^2\varphi + \sigma_{12}\sin 2\varphi + \sigma_{22}\sin^2\varphi - \sigma_{33}\right)\sin^2\psi \\ &\quad + \frac{1}{E}(\sigma_{33} - \nu\sigma_{11} - \nu\sigma_{22}) \\ &\quad + \frac{1+\nu}{E}(\sigma_{13}\cos\varphi + \sigma_{23}\sin\varphi)\sin 2\psi, \end{aligned} \tag{3}$$

where $\psi$ is the polar angle from the surface normal and $\varphi$ the azimuthal angle to the in-plane 1-axis; $E$ and $\nu$ are the Young modulus and Poisson ratio, respectively. In the presence of shear stresses $\sigma_{13}$ or $\sigma_{23}$ this gives rise to $\psi$ splitting (different values for $\pm\Psi$). For a biaxial stress field ($\sigma_{33} = \sigma_{23} = \sigma_{13} = 0$), it allows residual stress analysis by plotting $\varepsilon_{\varphi\psi}$ *versus* $\sin^2\psi$; for example, by tilting about the 2-axis ($\varphi = 0$) the in-plane stress $\sigma_{11}$ can be calculated from the slope of the curve:

$$\varepsilon_\psi = \frac{d_\psi - d^0}{d^0} = \frac{1+\nu}{E}\sigma_{11}\sin^2\psi - \frac{\nu}{E}(\sigma_{11} + \sigma_{22}). \tag{4}$$

The strength of this relation lies in the fact that it does not require a knowledge of the strain-free lattice spacing, since $d^0$ can be replaced in the denominator by $d_{\psi=0}$ without significant error because elastic strains are typically less than 1%, so that $d^0 \simeq d_{\psi=0}$. Of course, in reality, the grains in a polycrystal are not intrinsically elastically isotropic. As a result, equations (3) and (4) are not strictly valid and must be modified. There is not space here to embark on a detailed discussion of the effects of intrinsic and macroscopic elastic anisotropy on lattice strains, but it is covered in detail elsewhere (Welzel *et al.*, 2005). In essence, in the case of a macroscopically isotropic polycrystal, equation (4) can be modified by replacing $E$ and $\nu$ by their diffraction specific variants $E_{hkl}$ and $\nu_{hkl}$ or equivalently $S_1$ ($= -\nu_{hkl}/E_{hkl}$) and $S_2/2$ [$= (1+\nu_{hkl})/E_{hkl}$)]. For a macroscopically elastically anisotropic polycrystalline sample diffraction X-ray stress factors must be applied (Welzel *et al.*, 2005).

Recently, the penetrative power of neutrons and synchrotron X-ray radiation have extended the traditional range of its application from the surface to the bulk, provided that the condition of biaxiality is maintained (Hutchings *et al.*, 2005; Fitzpatrick & Lodini, 2003). The $\sin^2\psi$ method can appear in a number of guizes, *e.g.* whereby the unit-cell extrapolation is achieved using the minimum of inclinations or in a uniaxial equivalent. They are discussed in the following sections.

**4.6.1. $\sin^2\psi$ stress measurement methods**. For the conventional $\sin^2\psi$ technique (*e.g.* Noyan & Cohen, 1987) the biaxial stress assumption means that it is not necessary to calculate or measure the actual strain-free lattice spacing at all. For X-rays, because of the poor penetration, the method is used in back-scattered reflection geometry and the $\psi$ angles available usually extend from 0 to around 55°. In the X-ray case, depth profiling requires careful layer removal; it can also be applied nondestructively using neutron diffraction.

A good example is provided by carburizing, which is often used to surface harden steels; case depths vary depending upon application, but 0.4 mm is typical. The process involves the diffusion of carbon into the steel from a carbon-rich environment, by gas carburizing using a gas rich in CO, or pack carburizing using charcoal or coke with alkali carbonates bound together by oil or tar. Because the lattice parameter of steel is particularly sensitive to changes in C concentration (§3.1), use of a global strain-free lattice parameter would lead to very misleading conclusions about the state of stress near the surface. Carburizing can also introduce type II strains and stresses (Stickels & Mack, 1986). Great care therefore needs to be exercised in analysing measured strain data from carburized layers.

The application of the $\sin^2\psi$ method together with the assumption of zero out-of-plane stress circumvents the need to find the strain-free lattice parameter of the steel as a function of depth through the carburized layer. Measurements have been made in this way using both neutrons and X-rays (Bourke *et al.*, 1998). Fig. 8(*a*) shows the residual stress profiles thus determined. The X-ray profile was obtained by electropolishing the surface and subsequently correcting for layer removal. In view of the very shallow penetration depth characteristic of X-rays, the biaxial assumption is certainly valid for the latter and appears to be a good approximation for the former too. In the region very close to the surface (0–50 μm) the X-ray measurements have a unique advantage, but at greater depths the neutron results are more informative as well as being nondestructive.

The high penetrations available with high-energy synchrotron X-ray diffraction open up the possibility of using the $\sin^2\psi$ method over a wider range of $\Psi$ angles than is available for laboratory X-rays. In fact, the low scattering angles ($2\theta$) characteristic of high-energy X-rays mean that low $\psi$ angles

cannot be accessed in reflection because of the high path lengths associated with the glancing angles. Of course, in such a case the method still relies on the fact that the out-of-plane stress must be zero through the thickness of the plate, or if the sampling gauge spans the entire thickness it assumes that the local through thickness stresses average to zero (which is usually true for plates). A good example is provided by the mapping of the axial stress across a friction stir weld butt joint between non-age-hardenable AA5083 and age-hardenable AA6082 alloys supplied as 3 mm-thick plates 150 mm long and 60 mm wide (Fig. 8*b*). In this case, the $\sin^2\psi$ method was used (with $\theta = 4.8^\circ$ and $\psi$ varied from 45 to 90° using five $\psi$ tilts) to account for variations in $a^0$ across the welded plate (Steuwer *et al.*, 2006). These changes were extensive because of the different alloy chemistry of the two alloys being joined.

**4.6.2. $d^0$ inferred from $\sin^2\psi$ measurements near surface.** Equilibrium requirements mean that the stress normal to an unrestrained surface must always be zero. At the low surface penetrations characteristic of laboratory X-rays (tens of micrometres or less), an in-plane biaxial stress field ($\sigma_{33} = 0$) can normally be assumed.

A method proposed by Hauk *et al.* (1982) uses the fact that for a bi-axial stress state, at some angle $\psi^*$, the $d$ spacing will be equal to $d^0$. Inserting this into equation (3) allows the determination of $\psi^*$:

$$\sin^2\psi* = \frac{\nu/E}{(1+\nu)/E}\left(1+\frac{\sigma_{22}}{\sigma_{11}}\right) = \frac{\nu}{(1+\nu)}\left(1+\frac{m_2}{m_1}\right), \quad (5)$$

where $m_1$ and $m_2$ are the gradients of $d$ *versus* $\sin^2\psi$ plots at $\varphi = 0$ and 90°. $d^0$ is then simply the value of $d$ recorded at $\psi^*$ for $\varphi = 0$ (see Figs. 9*a* and 9*b*). This method has been used in Fig. 9(*c*) to measure the change in strain-free lattice parameter over the carburized depth discussed in the previous section (Bourke *et al.*, 1998) and for which the corresponding stress profile is shown in Fig. 8(*a*).

A related approach is to determine $d^0$ from the relation (Barrett & Massalski, 1966)

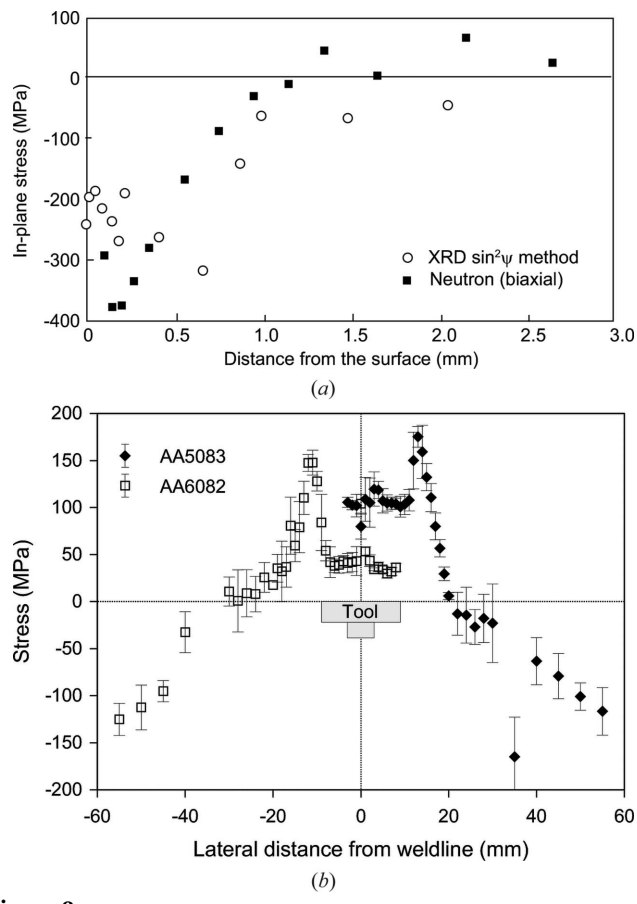


**Figure 8**
Measurement of stress using the bi-axial stress assumption. (*a*) Variation of the in-plane component of residual stress through a carburized layer on a 5120 steel disc as measured by neutron diffraction non-destructively and by X-ray diffraction (XRD) with layer removal using the $\sin^2\psi$ method (Bourke *et al.*, 1998). (*b*) Variation in the longitudinal residual stress as a function of distance from the weld line in a dissimilar AA5083/AA6082 aluminium alloy weld with AA5083 on the advancing side (positive $y$). The data were obtained using synchrotron X-rays at beamline ID32 at the ESRF (Steuwer *et al.*, 2006).

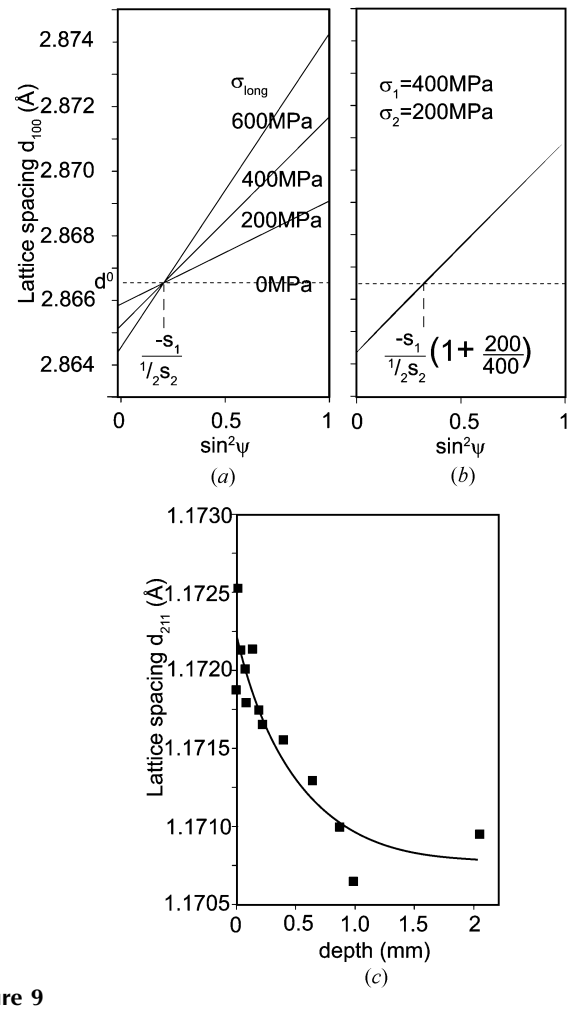


**Figure 9**
The strain-free lattice points $d^0_{100}$ for (*a*) uniaxial and (*b*) biaxial stress states calculated for the $d_{100}$ iron peak using equation (5) (Hauk & Kruger, 2000). (*c*) The strain-free lattice parameter $d^0_{211}$ variation with depth calculated in this manner for the carburized layer on 5120 steel for which the corresponding stress profile is shown in Fig. 8(*a*) (Bourke *et al.*, 1998).

$$d^0 = \left(\frac{\nu}{1+\nu}\right)\frac{d_{\varphi\psi} + d_{\varphi'\psi} - 2d_{\perp}}{\sin^2\psi} + d_{\perp}, \qquad (6)$$

where $d_{\varphi\psi}$ and $d_{\varphi'\psi}$ are the $d$ spacings measured at a polar angle $\psi$ from the surface normal and at azimuthal angles $\varphi$ and $\varphi' = \varphi + 90^\circ$ to the in-plane $x$ axis, and $d_\perp$ denotes the value of the $d$ spacing in the direction normal to the surface. Note that both equations use the fact that the trace of the biaxial stress tensor is invariant under rotation of axes so that $(\sigma_\varphi + \sigma_{\varphi'}) = (\sigma_{11} + \sigma_{22})$ is independent of the actual azimuthal $\varphi$ angle chosen and knowledge of the principal in-plane stress directions is not required (Barrett & Gensamer, 1936; Barrett & Massalski, 1966). To improve accuracy, measurements can be made at a number of $\psi$ angles to obtain, by analogy to the traditional $\sin^2\psi$ method, a more representative value. At first glance, it would appear that Poisson's ratio $\nu$ is generally not known with sufficient accuracy to apply equation (6) for the precise measurement of $d^0$; however, the first term is a small addition to the second, and so the method can normally give a value of $d^0$ that is accurate enough to be used to determine the strain.

Fig. 10 shows the variation in the strain-free lattice parameter against axial distance from the weld line obtained from the biaxial $\sin^2\psi$ measurement for a joint formed by inertia welding two 8 mm-wall-thickness tubes of RR1000 Ni base superalloy. It is also clear that in the near weld zone sharp gradients in $\gamma'$ precipitate microstructure occur. These are associated with the dissolution of $\gamma'$ during welding and the partial reprecipitation. In view of this it is not surprising that the strain-free lattice parameter varies considerably over the first 2–3 mm from the weld line. Note how the lattice parameter variation is largely independent of the radial position, varying only as a function of axial distance.

**4.6.3. $d^0$ inferred from measurements on thin slices**. A thin slice cut from a sample will tend to be in a condition of plane stress with the normal component averaging to zero through thickness ($\sigma_{33} = 0$). As a result the $\sin^2\psi$ technique can be applied using either neutron transmission (Santisteban *et al.*, 2002) or synchrotron X-ray diffraction techniques (Steuwer *et al.*, 2007) to map $d^0$. Following equation (6) a series of measurements are made at different $\psi$ tilts, at each of two angles $\varphi$ and $\varphi_{+90}$. This method is particularly well suited to the examination of thin slices using a pixellated time-of-flight neutron transmission detector. The experimental setup on the ENGIN instrument at ISIS is shown in Fig. 11, where the angles $\varphi$ and $\psi$ are indicated (Santisteban *et al.*, 2002). Instead of using the Bragg reflections, the Bragg edges are used. These correspond to drops in the transmitted signal where intensity is diffracted out of the transmission beam. These sharp edges in the straight through beam are recorded at each angle and can be fitted individually, or using a Rietveld-like multiple peak fit, enabling the corresponding $d^0$ or $a^0$ values to be

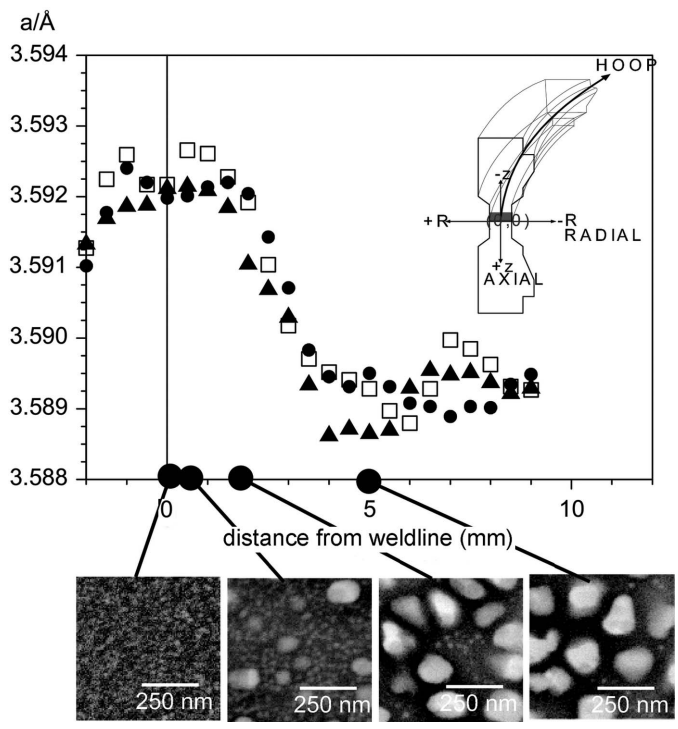


**Figure 10**
The variation in strain-free lattice parameter with distance from the weld centre line ($z$ = 0) for two RR1000 Ni superalloy tubes (wall thickness 8 mm) joined by inertia friction welding (Preuss *et al.*, 2002) near the inner (circles), centre (squares) and outer (triangles) radii. Also shown inset is the tube geometry and scanning electron images of the microstructure 0, 0.5, 2 and 9 mm from the weld line.

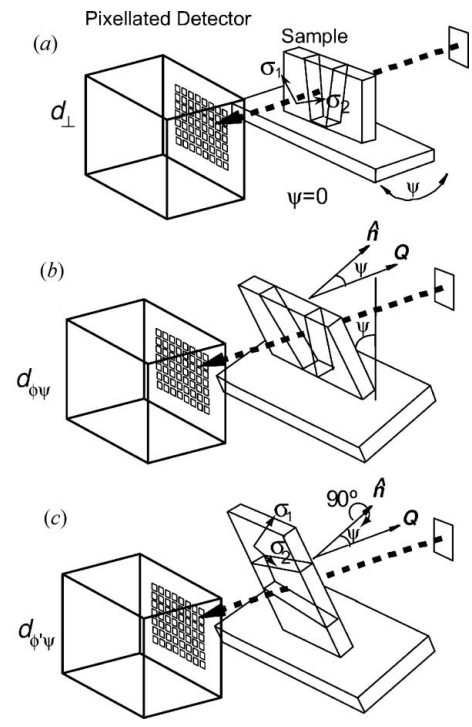


**Figure 11**
Schematic showing the setup for a two-dimensional full-field measurement of $d^0$ on a weld sample by transmission using the $\sin^2\psi$ method on the ENGIN instrument at ISIS. Two orthogonal axes must be used for the $\sin^2\psi$ tilts as shown by rotating 90° about $\hat{\boldsymbol{n}}$, but since it is not necessary for these to have special relationship to the in-plane principal axes it is possible to map $d^0$ with no prior knowledge, even when the in-plane stress field is complex (Santisteban *et al.*, 2002).

determined using in equation (5). Since the transmission spectrum obtained by each pixel corresponds to a different location, an image of the lattice parameter can be obtained.

An example of the method is provided by the mapping of $a^0$ across a slice taken from a ferritic weldment, used as a round robin sample in the VAMAS TWA20 programme. A number of samples were cut from a weld laid down by TWI, UK, in a 6 mm-wide 8.5 mm-deep U-groove machined in the middle of a BS 4360 50D ferritic steel plate 1000 × 150 × 12.5 mm in size. The groove was filled by a 12-pass mechanized tungsten inert gas weld. A 3 mm-thick 40 mm-long slice was electro-discharge machined from the 12.5 mm-thick plate and weldment for transmission measurements. This slice was placed in front of a two-dimensional pixellated detector comprising a 10 × 10 array of 2 × 2 mm scintillation detectors on a 2.5 mm pitch (Santisteban *et al.*, 2002) and tilted around the transverse (TD) and short transverse (STD) directions of the original plate, as shown in Fig. 12(*a*). $\psi$ angles of 0, 18.4, 24.4 and 28.4° were used for the definition of the slopes of the $a_\psi$ *versus* $\sin^2\psi$ graph. Relatively low angles were chosen in order to minimize excessive distortion of the mapped area. In this manner a map of $a^0$ has been obtained (Fig. 12*a*). The map resembles the shape of the weld but is asymmetric relative to the weld centre line, presumably as a result of the asymmetric welding sequence. The extent of the lattice parameter variation found was equivalent to 600 × $10^{-6}$. Neglecting this difference and assuming a single global value for $a^0$ would introduce an error of 130 MPa in the residual stress, which is of the same order of magnitude as typical stresses found in practice.

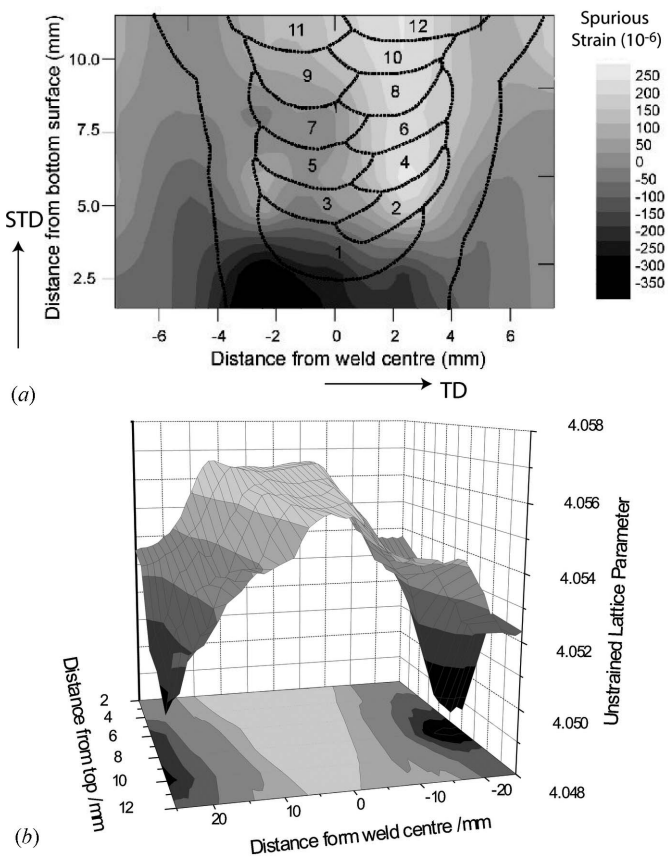


**Figure 12**
(*a*) Interpolated map of the unstressed lattice parameter $a^0$ measured on a thin (2 mm) slice for a ferritic weld. The change in $a^0$ is expressed in terms of a spurious strain relative to the value far away from the weld, in the parent material (Santisteban *et al.*, 2002). (*b*) The variation of the unstrained lattice parameter calculated from the measured 311 lattice plane spacings measured by synchrotron X-rays using equation (1) for a thin cross-sectional slice of an AA7010 friction stir weld (Steuwer *et al.*, 2007).

The $\sin^2\psi$ analysis can also be carried out quickly and effectively on excised cross-sectional slices using high-energy synchrotron X-ray diffraction using low scattering angles in transmission. A good example is provided by the accurate measurement of the local variation in lattice parameter across a friction stir weld (FSW) of a 13 mm-thick Al 7010 (5.7–6.7% Zn, 2.1–2.6% Mg, 1.5–2.0% Cu, 0–0.12% Si, 0–0.15% Fe, 0–0.10% Mg, 0–0.05% Cr, 0.10–0.16% Zr) plate (Steuwer *et al.*, 2007). This was undertaken using a rotational speed of 270 r.p.m., traverse speed 81 mm $min^{-1}$, with a vertical (downward) force of approximately 36 kN. The tool had a 18 mm-diameter shoulder and an M5 threaded pin 5 mm wide and 0.8 mm pitch. Since the unstrained lattice parameter of aluminium varies markedly with the solution of other elements (as shown in Fig. 1) it is essential that the variation in strain-free lattice parameter is accounted for in stress measurements. A 1 mm-thick cross-sectional slice was cut midway along the FSW in order to use the transmission $\sin^2\psi$ method, and the variation in $d^0$ is mapped across the weld in Fig. 12(*b*). It is evident that the changes in strain-free lattice parameter are significant. Note that the variation in lattice parameter has the same shape as the Vickers hardness (Steuwer *et al.*, 2007). Age hardening alloys are particularly prone to changes in solute content with precipitation; if a single global value of $d^0$ were used as reference in this case it would give a spurious strain of up to 2000 × $10^{-6}$, corresponding to an error in stress of up to 140 MPa. It is clear that were the variation in stress-free lattice parameter not taken into account the tensile strains near the weld centre line would be significantly underestimated.

**4.6.4. Analysis of complete Debye–Scherrer cones**. It is now possible to collect complete diffraction rings at the low diffracting angles characteristic of high-energy synchrotron X-ray beamlines using CCD cameras. Strain results in the distortion of the ideal circular Debye–Scherrer cone into an ellipse. This fact suggests the idea of using the complete ring pattern as the data set to be fit with an ellipse described by the three parameters: the major and minor semi-axes, and the orientation angle (Korsunsky *et al.*, 1998). Unfortunately, in early work distortion associated with the CCD detector was found to be too large to allow efficient correction for the present purposes, when reliable strain values need to be extracted with the accuracy of less than 100 × $10^{-6}$. Wanner & Dunand (2000) used an iron reference powder attached physically to the sample to correct for any change in the camera length or distortion of the CCD camera. In studying uni-axial deformation of Cu–Mo composites they used the fact that the major and semi-major axes are parallel and perpendicular to the applied stress to plot a $\sin^2\varphi$ plot by analogy to

conventional $\sin^2\psi$ plots from which they were able to extract the change in the axial and transverse phase stresses (Fig. 13). Because biaxial in-plane stress would give an isotropic increase/decrease in the ring radius indistinguishable from a larger/smaller strain-free lattice spacing it is only possible to determine the relative changes in strain without sampling an out-of-plane component of lattice spacing. This could be achieved by using the fact that diffraction rings sample successively larger values of $\psi$, but has not been exploited to date.

### 4.7. Option 6: imposing stress and moment balance

An approach to the determination of reference $d$ spacings, which precludes the need for their measurement, is to adopt the fundamental continuum mechanics-based requirements that force and moment must balance across selected cross sections of the sample. The approach is to measure the required field of $d$ spacings, or diffraction angles, in the sample and, using a nominal $d_{\rm ref}$, to calculate the strain and stress in the sample. Subsequently the reference value is varied iteratively in order to infer the true reference value, that is the value that renders a stress field in which force and moment balance occurs. In adopting this approach great care must be taken in selecting appropriate cross sections over which to require the forces and moments to balance. It must be ensured that the experimental data set covers the entire cross section and not just a part of it, and also that a single global value of $d_{\rm ref}$ is appropriate.

In practice, this method is probably best held in reserve to check the validity of the $d^0$ value obtained from one of the other methods listed above. Indeed when applicable, its use as a check of the validity of a measured stress field is recommended. A good example is provided by an analysis of the inertia welded tube described in §4.6.2. In view of the fact that the weld microstructure was very similar from the inside to the outside of the tube (varying only with distance from the weld $z$) it is possible to apply stress balance across the wall thickness of the tube and thereby to infer the lattice parameter as a function of axial distance ($z$). The results of this analysis are shown in Fig. 14($a$). As can be seen, excellent agreement for the as-welded sample was obtained between both $a^0$ correction methods. Note also that after post-weld heat treatment (PWHT; Fig. 14$b$) the gradients in solute concentration responsible for the lattice parameter changes disappear owing to reprecipitation, such that a single global value of the strain-free lattice parameter is sufficient.

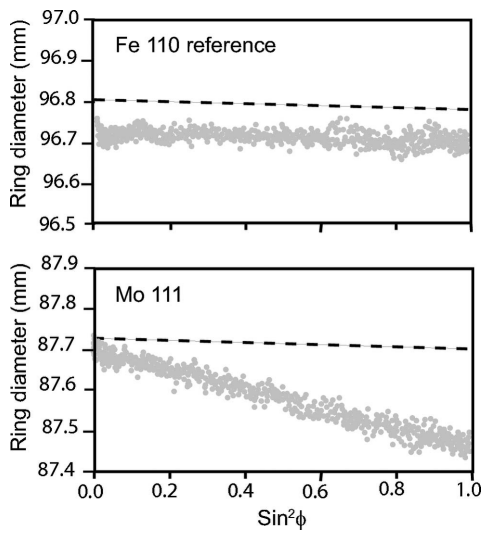


**Figure 13**
Plots of $d$ *versus* $\sin^2\varphi$ of Mo 111 and reference Fe 110 diffraction rings recorded for a Cu–Mo composite loaded *in situ* to 236 MPa tensile stress. The dashed lines in the latter diagrams are best linear fits to the corresponding data from the unloaded specimen.

## 5. Composite materials

It can be difficult to obtain a reliable measure of the respective stress-free lattice spacings when considering multiphase materials and composites. In such cases it is unlikely that any phase in the composite will be stress-free. With regard to making useful measurements on such materials, one needs to consider whether the macrostress variation or the individual average phase stresses are important. Except in the elastic case, or when the secondary phases are very dilute, no single phase alone can provide a picture of the macroscopic residual stress, since the (continuum) macrostress is given by the sum of the individual phase stresses. If one is interested in the macrostress the corresponding strain-free lattice parameters are needed for all significant phases to determine average stress in each phase $\sigma_i$ of fraction $f_i$, giving

$$\sigma^{\rm macro} = f_1\sigma_1 + f_2\sigma_2 + \cdots. \qquad (7)$$

In some cases a successful strategy is to obtain the strain-free lattice spacing representative of a phase in a composite, *e.g.* by chemically isolating the fibres in a composite (Preuss *et al.*, 2003) or by etching the ferrite matrix to reveal the austenite phase in a duplex steel (Johansson *et al.*, 1999), but the second phase may be more difficult. In such circumstances it may be possible to infer the appropriate strain-free lattice parameter in the second phase by using the overall stress balance criterion of equation (7). In cases where the temperature is

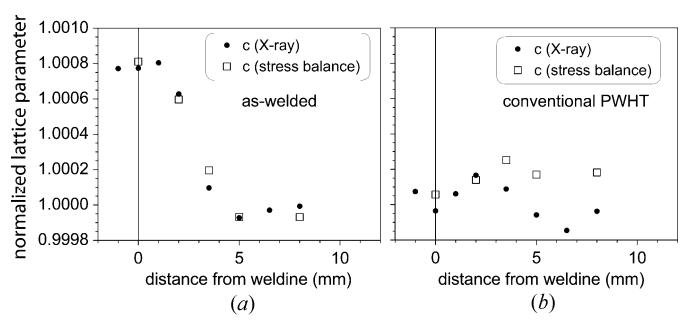


**Figure 14**
The fractional change in lattice parameter relative to the parent value with distance from the weld centre line of the inertia weld shown in Fig. 8 using the X-ray method (full symbols) of §4.6.2 and deduced by applying stress balance across the wall thickness (open symbols) ($a$) after welding and ($b$) subsequent to heat treatment.

varied the strain-free lattice spacing must be either measured as a function of temperature (Withers *et al.*, 1987) or predicted on the basis of that at room temperature and the relevant expansion coefficient. In many cases, absolute stress levels are not reported but rather changes that take place, for example during deformation (Wanner & Dunand, 2000). In such cases it should be remembered that thermal residual stresses or other pre-existing residual stresses may mean that the absolute stresses are significantly different from those reported. This is well illustrated by the fragmentation of a single SiC fibre in a Ti matrix (Bennett *et al.*, 2005) (Fig. 15). Here the locations at which fibre breakage had occurred were subsequently taken to be strain-free. On this basis, it can be seen that elastic fibre strain in the undeformed sample is compressive along the whole of the gauge length. The residual compressive strain varies along the gauge length and is highest between $z = 3$ and $z = 5$ mm, reaching a maximum of around $-3200 \times 10^{-6}$ (around $-1.3$ GPa). This residual strain arises as a consequence of the thermal expansion misfit between the fibres and matrix generated as a result of the processing temperature (1173 K), the opportunity for stress relaxation during cooling and the volume fractions of each phase. If the difference in coefficient of thermal expansion between the phases is around $6 \times 10^{-6}$ K then the residual strain is equivalent to a temperature drop of around 803 K. This is essentially the increment in temperature $\Delta T_{\rm esf}$ required to make the composite effectively stress-free. The variability of residual stress along the length of the fibre is almost certainly due to the fabrication process. Failure to take account of the compressive thermal residual fibre stresses would suggest a fibre fracture strain that is some 2000–3000 $\times 10^{-6}$ (>1 GPa) more tensile than is the case.

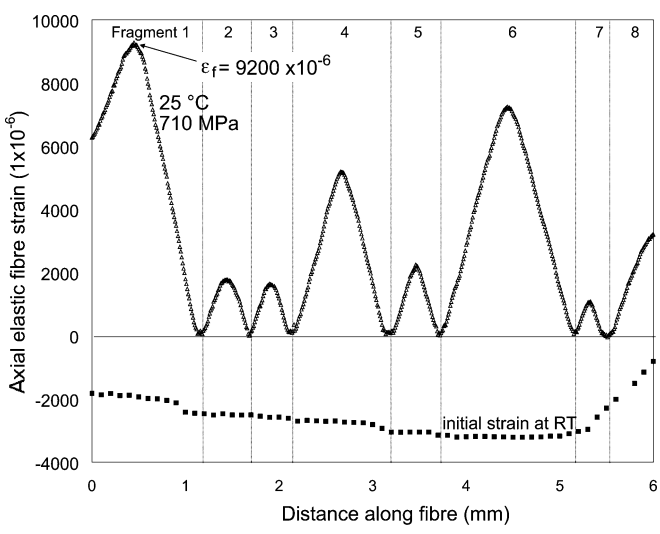


**Figure 15**
Variation of axial elastic fibre strain, $\varepsilon_f$, measured along a 140 µm-diameter SCS6 SiC fibre embedded in a Ti–6Al–4V matrix, prior to and after fibre fragmentation at room temperature (RT) using 75 keV synchrotron X-rays with 10 × 200 µm slits (along $x$ normal to the fibre). The squares show the residual strains recorded before loading and the triangles were recorded at a load of 710 MPa (Bennett *et al.*, 2005).

## 6. Conclusions

In this paper some well established, as well as some relatively new options for obtaining a best estimate for the appropriate strain-free reference lattice spacing have been reviewed and examples of their application given. On the whole, great care and judgement needs to be exercised when choosing an appropriate and cost-efficient method. The following observations can be made.

(i) If there is any suspicion that the strain-free lattice parameter may vary from place to place, then local methods must be used, if only to demonstrate that the application of a global measure of the strain-free lattice spacing is appropriate.

(ii) The uncertainty in $a^0$ affects all measurements of elastic strain; too often, too little time and effort is spent determining $a^0$ given that any error propagates through all the calculations of elastic strain and stress. It is recommended that ten times the measurement time is allocated to the measurement of $a^0$ if a global value is being used. Alternatively, repeat measurements of $a^0$ can be used to give better statistics.

(iii) If a global value of $d^0$ is adopted, the corresponding measurement uncertainty should not be combined in quadrature with that associated with each point in turn since it affects all points similarly.

(iv) The experimenter must decide whether the macrostress component only is required, or the average stress in the phase or grain family, and the strategy for measurement chosen accordingly.

(v) Imprecise positioning of reference samples can lead to geometrical effects which affect measurement accuracy, or lead to measurements that are not representative of the strain measurement locations.

(vi) Too often basic assumptions about the state of stress, or the effects of previous processing on the region of interest, are not justified, leading to inappropriate deduction of the reference spacing.

(vii) If at all possible the overall balance of stress and moment should be reserved to test the integrity and validity of the measurements, once the stresses have been mapped, using other methods to obtain the strain-free lattice parameter.

(viii) The effects of phase transformations, thermal effects, texture and plasticity can all affect the representativeness of strain-free measurements.

(ix) Mixed strategies whereby deep measurements of lattice spacing in engineering components are made using neutrons or high-energy synchrotron X-rays supplemented by strain-free measurements of the reference lattice spacing using laboratory-based analysis of slices or cubes can be a cost-effective solution.

(x) It is recommended that for cubes the whole sample is bathed in the beam in case there are stresses within them, but this requires meticulous positioning to avoid geometrical surface effects that can drown out other lattice parameter changes.

(xi) Multiple measurements at different locations through thickness or with position are advisable if using the far-field

method to ensure that the locations chosen are really macrostress-free.

PJW acknowledges the support of a Royal Society Wolfson Merit Award. The authors are grateful to those maintaining and supporting the neutron and synchrotron X-ray facilities around the world at which the measurements described here were taken, as well as those who took part in the VAMAS TWA20 expert group of stress measurement by diffraction.

## References

Barrett, C. S. & Gensamer, M. (1936). *Physics*, **7**, 1.
Barrett, C. S. & Massalski, T. B. (1966). *Structure of Metals*. Oxford: Pergammon.
Bennett, J. A., Preuss, M. & Withers, P. J. (2005). International Conference on Composite Materials (ICCM) 15, Durban, South Africa.
Bhadeshia, H. K. D. H., David, S. A., Vitek, J. M. & Reed, R. W. (1991). *Mater. Sci. Technol.* **7**, 686–698.
Bourke, M. A. M., Rangaswamy, P., Holden, T. M. & Leachman, R. (1998). *Mater. Sci. Eng. A*, **257**, 333–340.
Ceretti, M., Coppola, R., Di Pietro, E. & Nardi, C. (1998). *J. Nucl. Mater.* **263**, 1005–1009.
Clausen, B., Lorentzen, T., Bourke, M. A. M. & Daymond, M. R. (1999). *Mater. Sci. Eng. A*, **259**, 17–24.
Daymond, M. R., Bourke, M. A. M., Von Dreele, R. B., Clausen, B. & Lorentzen, T. (1997). *J. Appl. Phys.* **82**, 1554–1556.
Daymond, M. R. & Johnson, M. W. (2001). *J. Appl. Cryst.* **34**, 263–270.
Durer, A. (1946). *Z. Metallkd.* **37**, 60.
Eigenmann, B. & Macherauch, E. (1995). *Materialwiss. Werkstofftech.* **26**, 148–160.
Fitzpatrick, M. E. & Lodini, A. (2003). Editors. *Analysis of Residual Stress by Diffraction using Neutron and Synchrotron Radiation*. London: Taylor and Francis.
Gloaguen, D., François, M. & Guillen, R. (2004). *J. Appl. Cryst.* **37**, 934–940.
Glocker, R. (1951). *Z. Metallkd.* **42**, 122–124.
Hauk, V. (1997). *Structural and Residual Stress Analysis by Non-destructive Methods*. Oxford: Elsevier Science.
Hauk, V. & Kruger, B. (2000). *Mater. Sci. Eng. A Struct. Mater.* **284**, 261–267.
Hauk, V. M., Oudelhoven, R. W. M. & Vaessen, G. J. H. (1982). *Metall. Trans. A*, **13**, 1239–1244.
Hutchings, M. T., Bouchard, P. J. & Withers, P. J. (2000). *Characterization of the Residual Stress State in a Double 'V' Stainless Steel Cylindrical Weldment Using Neutron Diffraction and Finite Element Simulation*, 6th International Conference on Residual Stress, edited by G. A. Webster. Oxford: Institute of Materials.
Hutchings, M. T., Withers, P. J., Holden, T. M. & Lorentzen, T. (2005). *Introduction to the Characterization of Residual Stresses by Neutron Diffraction*. London: CRC Press, Taylor and Francis.
Johansson, J., Oden, M. & Zeng, X.-H. (1999). *Acta Mater.* **47**, 2669–2684.
Johnson, M. W. (2005). Private communication.
Johnson, M. W., Edwards, L. & Withers, P. J. (1997). *Physica B*, **234**, 1141–1143.
Korsunsky, A. M., Wells, K. E. & Withers, P. J. (1998). *Scr. Mater.* **39**, 1705–1712.
Krawitz, A. D. & Winholtz, R. A. (1994). *Mater. Sci. Eng. A Struct. Mater.* **185**, 123–130.
Mohr, A. & Priesmeyer, H. G. (1995). *Proc. SPIE*, **2339**, 350–355.
Noyan, I. C. & Cohen, J. B. (1987). *Residual Stress – Measurement by Diffraction and Interpretation*. New York: Springer-Verlag.
Nye, J. F. (1985). *Physical Properties of Crystals – Their Representation by Tensors and Matrices*. Oxford: Clarendon.
Pang, J. W. L., Holden, T. M. & Mason, T. (1998). *Acta Mater.* **46**, 1503–1518.
Preuss, M., Pang, J., Withers, P. J. & Baxter, G. J. (2002). *Metall. Mater. Trans. A*, **33**, 3215–3225.
Preuss, M., Rauchs, G., Doel, T., Steuwer, A., Bowen, P. & Withers, P. J. (2003). *Acta Mater.* **51**, 1045–1057.
Santisteban, J. R., Steuwer, A., Edwards, L., Withers, P. J. & Fitzpatrick, M. E. (2002). *J. Appl. Cryst.* **35**, 497–504.
Steuwer, A., Dumont, M., Peel, M., Preuss, M. & Withers, P. J. (2007). *Acta Mater.* **55**, 4111–4120.
Steuwer, A., Peel, M. J. & Withers, P. J. (2006). *Mater. Sci. Eng. A*, **441**, 187–196.
Stickels, C. A. & Mack, C. M. (1986). *J. Heat Treat.* **4**, 223–236.
Wanner, A. & Dunand, D. C. (2000). *Metall. Mater. Trans. A*, **31**, 2949–2962.
Webster, G. A. (2001). Editor. *Polycrystalline Materials – Determinations of Residual Stresses by Neutron Diffraction*. ISO/TTA3 Technology Trends Assessment, Geneva 20, Switzerland.
Welzel, U., Freour, S. & Mittemeijer, E. J. (2005). *Philos. Mag.* **85**, 2391–2414.
Withers, P. J., Jensen, D. J., Lilholt, H. & Stobbs, W. M. (1987). *The Evaluation of Internal Stresses in a Short Fibre Metal Matrix Composite by Neutron Diffraction*, *Proceedings of ICCM VI/ECCM2*, edited by F. L. Matthews, N. C. R. Buskell, J. M. Hodgkinson & J. Morton. London: Elsevier.
Withers, P. J., Johnson, M. W. & Wright, J. S. (2000). *Physica B*, **292**, 273–285.